Biomedical Signal Processing and Control 51 (2019) 73–81

Contents lists available at ScienceDirect

Biomedical Signal Processing and Control

journal homepage: www.elsevier.com/locate/bspc

Improved parallel MR imaging with accurate coil sensitivity estimation using iterative adaptive support

Jinhua Sheng [a,*,1], Bocheng Wang [a,b], Yangjie Ma [a], Qingqiang Liu [a], Weixiang Liu [a], Bin Chen [a], Meiling Shao [a]

[a] College of Computer Science, Hangzhou Dianzi University, Hangzhou, Zhejiang, China
[b] Communication University of Zhejiang, Hangzhou, Zhejiang, China

ARTICLE INFO

Article history:
Received 1 August 2018
Received in revised form 9 January 2019
Accepted 2 February 2019

Keywords:
Sensitivity maps
SC SENSE
Joint estimation
Penalty function
Parallel MRI

ABSTRACT

Estimation of sensitivity profile in SENSE-like methods plays a crucial role in reconstruction. The self-calibration of sensitivity eliminates the separate calibrating scan and therefore reduces imaging time. However, sensitivity estimation by zero-filling in each column outside region of the object introduces inaccuracy and artifacts into the results, especially for the image periphery. Noise and error may propagate to reconstruction. In this paper, based on the method of joint sensitivity estimation and image reconstruction, penalty theory was used to reformulate the objective function to refine the sensitivity maps in each coil. The proposed method was tested on various data sets and in vivo brain data were shown for comparison. By suppressing the background and enhancing sensitivity maps in the region of interest through iterations, the quality of reconstructed image improved significantly, especially when a rather large reduction factor was used.

1. Introduction

Parallel magnetic resonance imaging (pMRI) is a widely used technique using surface coils to reconstruct an image with reduced sampling and accelerated scanning. Different from the "regular" MRI, coils used in pMRI receive MR signals by a completely independent information process. In non-parallel imaging, signals are combined into an aggregate. The time of imaging is determined by the number of phase encoding steps due to its full sampling pattern. pMRI becomes practical because of the effectiveness of reducing cost of the MRI. But, reduced sampling in k-space results in different kinds of artifacts during reconstruction. Aliasing is the most serious one that has to be resolved.

Over the past decades, a number of pMRI techniques were proposed addressing the problem. All of them generally fall into two strategies: the image domain based and the k-space domain based. Examples include simultaneous acquisition of spatial harmonics (SMASH) [1], sensitivity encoding (SENSE) [2] and sensitivity profiles from an array of coils for encoding and reconstruction in parallel (SPACE-RIP) [3]. These all require explicit sensitivity profile to reconstruct the image. Meanwhile, other methods, such as partially parallel imaging with localized sensitivities (PILS) [4], generalized auto-calibrating partial parallel acquisition (GRAPPA) [5], do not need the coil sensitivity maps to be given. The most obvious difference between them lies in the sequence of calibration and reconstruction. The former strategy reconstructs aliasing images first and then unfolds artifacts, which provides a slightly higher signal to noise ratio (SNR) with increases of the reduction factor as long as the sensitivity estimated is accurate. The latter strategy fills data in missing lines in k-space first and then reconstructs the image. Both strategies require an extra estimation of sensitivity in image domain or self-calibration of k-space lines to calculate the necessary information before or after reconstruction. Scanning time is therefore prolonged which counteracts the original intention of pMRI.

In order to eliminate the separate scanning, auto-calibrating techniques were proposed. Auto-calibrating simultaneous acquisition of spatial harmonics (AUTO-SMASH) [6], variable-density AUTO-SMASH (VD-AUTO-SMASH) [7], self-calibrating parallel imaging with automatic coil sensitivity extraction (SC SENSE) [8] and ESPIRiT [9] were introduced to satisfy the requirement of sensitivity estimation by using the strategy of acquiring small numbers of center lines in k-space and naming those as auto-calibration signal (ACS) lines. ACS lines are used not only for sensitivity estimation, but also for participation in reconstruction as a part of the whole

* Corresponding author.
E-mail address: j.sheng@ieee.org (J. Sheng).
[1] Senior Member of IEEE

https://doi.org/10.1016/j.bspc.2019.02.001
1746-8094/

k-space data. Variable-density is a trajectory in sampling k-space with fully extracted inner portion in ACS and under sampled in the outer portion. This would be expected to sacrifice image quality and reduce SNR in reconstruction.

An iteration algorithm was introduced to enhance the accuracy of the sensitivity profile. Ying and Sheng proposed JSENSE [10] to effectively improve the imaging by jointly estimating coil sensitivity and the desired image. Based on SC SENSE, the reconstructed result was involved in the solving of sensitivity inversely. As a result, both of the sensitivity and the quality of reconstruction became gradually accurate by repeating the process. Polynomial fitting of sensitivity was also implemented in JSENSE to achieve smoothness and reduce noise [11], but a proper order of polynomial was hard to determine. Higher value caused overfitting with increased computing cost, while the lower value led to underfitting with no effect. The times of joint estimation also seriously affected the cost of imaging because it needed to complete the whole reconstruction process to update sensitivity for each coil in each iteration. Xie et al. [12] implemented JSENSE by using the multi-channel coil images instead of the reconstructed output. Uecker et al. [13] proposed an algorithm based on a Newton-type method with appropriate regularization terms in JSENSE to yield images. Chun et al. [14] extended the joint estimation to compressed sensing SENSE (CS SENSE).

In this paper, we propose a novel approach to improve the image quality in pMRI by estimating the sensitivity profile based on the prior knowledge that sensitivity outside the region of body interested for imaging makes little sense in the reconstruction. In regular process of SENSE-like, the corresponding column in the sensitivity matrix is removed and the excluded pixel is assigned zero in the final image [2]. While in SC SENSE, VD data are acquired in the center of k-space, the information used to estimate sensitivity is limited with the loss of high frequency. Thus, zero-filling column by column introduces more error into the low resolution maps. Meanwhile, the transilience of the sensitivity value at the edge of the object brings Gibbs-like artifacts somewhere in the final image. Inhomogeneity and noise in coils and space also make it impossible to detect outside the body. As a result, either large or small sensitivity values can always be observed in that region. Instead of zero-filling, we extend the objective function of sensitivity estimation by a penalty term to suppress noise outside and enhance the accuracy in the region of interest. Mathematically the penalty term is multiplied by a mask matrix which indicates the border of the interested region. The mask values in region of interest are assigned to 0, and others are set to 1. Optimal solving is achieved by iterations in this exterior penalty function. As a result, the useless information outside the body will be constantly suppressed and approached to zero during the iteration. In general, followed by the acquisition of ACS lines and the reconstruction of low resolution image using sum of squares (SoS), sensitivity profile is considered as an unknown to be solved with restrained in penalty. Compared to SC SENSE, the reconstruction results from a set of in vivo brain data are tested in this paper to demonstrate its superior quality.

2. Materials and methods

The proposed method was implemented in Matlab (Mathworks, Natick, MA). To validate its effectiveness in pMRI, in vivo data from a healthy volunteer were acquired with an eight channel head coil on a 3 T Excite MRI system (GE Healthcare Technologies, Waukesha, WI, USA) and gradient echo sequence (TE = 3.2 ms, TR = 2 s, FOV = 24 cm, matrix = 256 * 256, slice thickness = 5 mm). Informed consent was obtained from the volunteer in accordance with the institutional review board policy.

Intermediate images of full scan data in eight coils were first processed by sum of squares method to generate the SoS image as a standard reference. In SC SENSE, sensitivity maps estimation was accomplished by extracting center lines in phase encoding direction in k-space transformed by 2D FFT of the intermediate images, according to the ACS lines setting. To maintain the range of phase encoding bandwidth in k-space, other lines were filled with zeros. As a result of filling, there existed truncation effect (Gibbs ring) in the low resolution image reconstructed by sum of squares of each channel image inversely Fourier transformed from k-space data. In general, k-space apodization before transformation can be an effective method, although it is harmful to the resolution and quality of image reconstruction. Various window functions can be used. In this paper, Tukey window with parameters ($kc = 0$, w = ACS lines / 2) was adopted to alleviate the serious Gibbs artifacts. Other available windows like Kaiser can also be used [9,15]. A larger falling distance w would be beyond the scope of ACS lines and apodize with no effect, and a smaller one would make some information loss in k-space and reduce more quality of reconstruction. Fig.1 shows the k-space data with and without window processing. Because filling zeros appeared in the phase encoding direction and it was fully sampled in frequency encoding, the Tukey window was convolved with the vertical k-space data in each column in Fig. 1a. As a sample scenario to illustrate apodization, the 113th column in frequency encoding was marked in Fig. 1a–b and plotted in Fig. 1c–d.

Variable density data sets sampled in k-space make the actual accelerating speed (termed net reduce factor, R_{net}) not the same with expected reduction factor (termed nominal reduction factor, R_{nom}). ACS lines are extracted with full data while the others are under sampled according to R_{nom}. Therefore, the actual accelerating speed is usually less than the expected in the method:

$$\begin{aligned} SUM &= N^{ACSL} + \frac{N^{fully\ sampled} - N^{ACSL}}{R_{nom}} \\ R_{net} &= \frac{N^{fully\ sampled}}{SUM} \end{aligned} \tag{1}$$

The term of normalized mean squared error (NMSE) which is also referred to as artifact power (AP) in various literatures [16,17] measures the quality of pMRI. The formula is defined as the normalized difference square between the reconstructed image (I_{recon}) and the SoS as the standard reference (I_{sos}), and a higher value of NMSE represents increased noise in reconstruction:

$$NMSE = \sum_{i}^{CoilN} \frac{\left\| I_{recon}(i) - I_{sos} \right\|}{\left\| I_{sos} \right\|} \tag{2}$$

Artifact should be well considered during reconstruction of parallel MR image, especially for method SENSE-like. Each reconstruction result is followed by subtracting the SoS image for each pixel to obtain an equal scale difference maps which visually present where artifact appears and how serious the noise is.

An array of surface coils is used to reconstruct image in pMRI. Interlaced scan in each coil induces reduction of field of view (FOV), and whenever the scale of an object exceeds that, the so called wrap–around artifact occurs as one particular phenomenon of aliasing. In SENSE, pixels in aliasing images together with sensitivity maps contribute to reconstruct imaging. After the inverse Fourier transform, signal of each coil is processed to an intermediate image which is represented as vector $\mathbf{m}_i$ (shown in Fig. 2) and contains the complex values of superimposed pixels. Here i = 1,2,. . ., N^{coil} is the index of coils. Each $\mathbf{m}_i$ is assembled into a $N^{coil} \times 1$ matrix $\mathbf{m}$, which is equal to the combination of image F $\boldsymbol{f}$ ($n_p \times 1$) that needs to be solved and the encoding $N^{coil} \times n_p$ matrix $\mathbf{E}$, where the subscript p counts the number of superimposed pixels.

To take the simplest case as an example, in Fig. 3, when reduction factor is 2, each aliasing pixel in $\mathbf{m}_1$ is a superposition resulting from

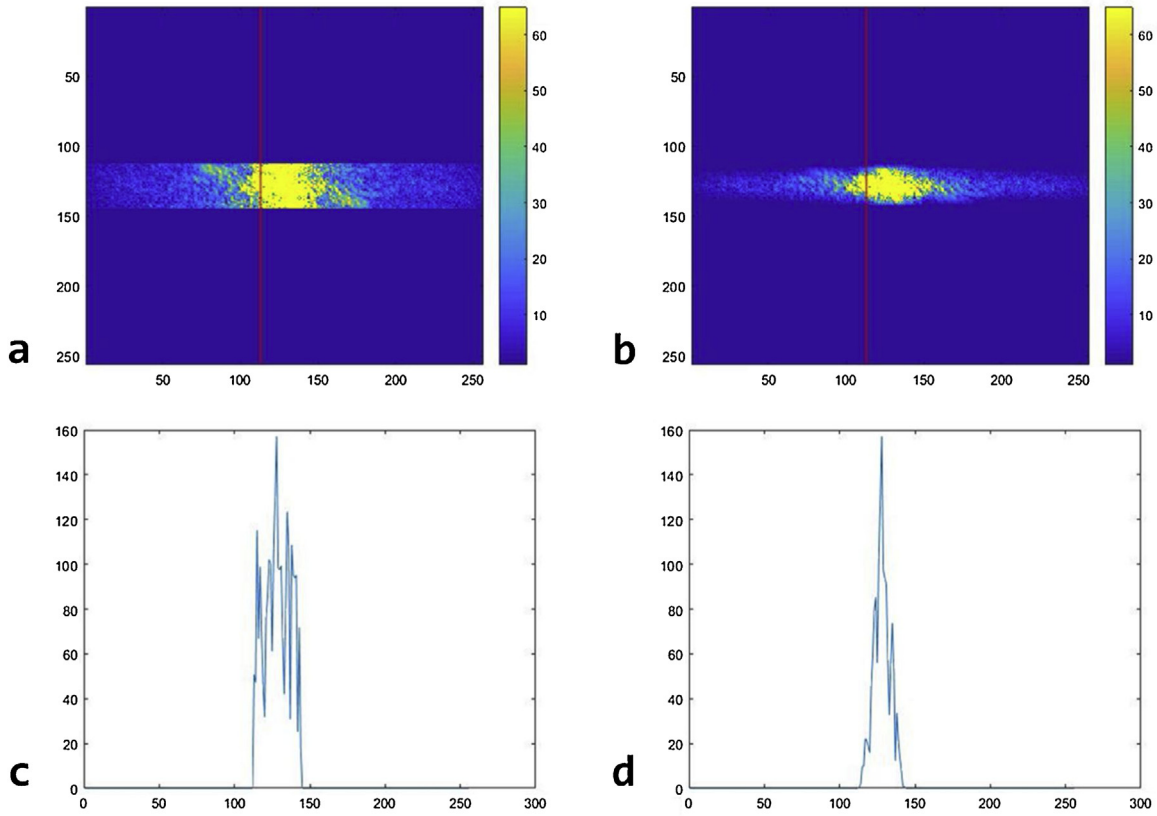

Fig. 1. K-space data comparison with and without window function processing. (a) k-space data before apodization, (b) k-space data convolved with window function, (c) amplitude of the 113th column in frequency encoding direction of k-space data before window, marked in red single line in (a), and (d) amplitude of the 113th column marked in (b) convolved with window function, which can be observed truncation was suppressed.

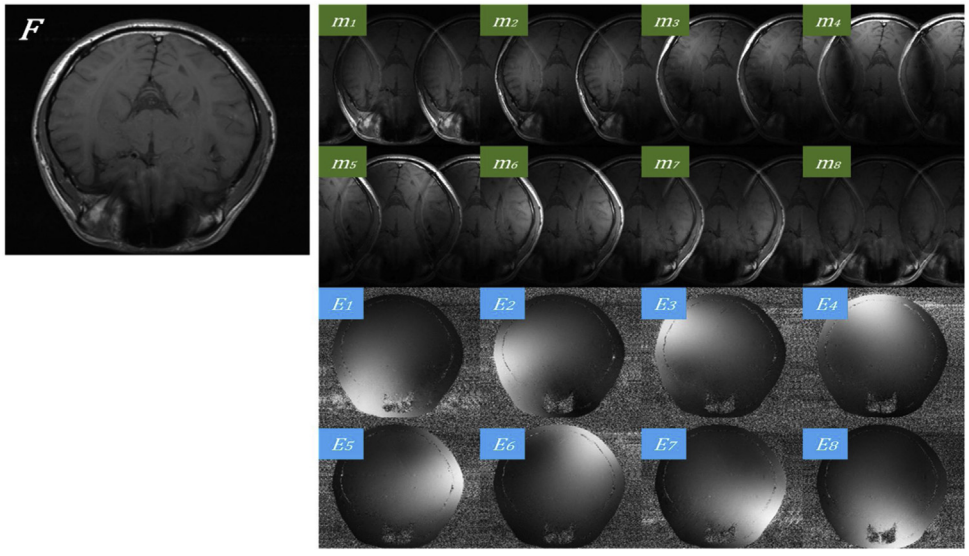

Fig. 2. Reconstruction image $\boldsymbol{f}$, sensitivity map $\mathbf{E}_i$ and aliasing image $\mathbf{m}_i$ in each coil.

two pixels in **F**. Considering position a. For coil#1, a pixel $m_{1,a}$ in $\mathbf{m}_1$ is the combination of $E_{1,a}{\cdot}f_a$ and $E_{1,b}{\cdot}f_b$, which is described in Eq. (3). For all coils, $m_{i,a}$ is the combination of $E_{i,a}\cdot f_a$ and $E_{i,b}\cdot f_b$, which is given by Eq. (4).

$$m_{1,a} = E_{1,a}\cdot f_a + E_{1,b}\cdot f_b \tag{3}$$

$$\boldsymbol{m_a} = \boldsymbol{E_a}\cdot\boldsymbol{f_a} \longleftarrow \begin{cases} m_{1,a} = E_{1,a}\cdot f_a + E_{1,b}\cdot f_b \\ m_{2,a} = E_{2,a}\cdot f_a + E_{2,b}\cdot f_b \\ \cdot \\ \cdot \\ \cdot \\ m_{8,a} = E_{8,a}\cdot f_a + E_{8,b}\cdot f_b \end{cases} \tag{4}$$

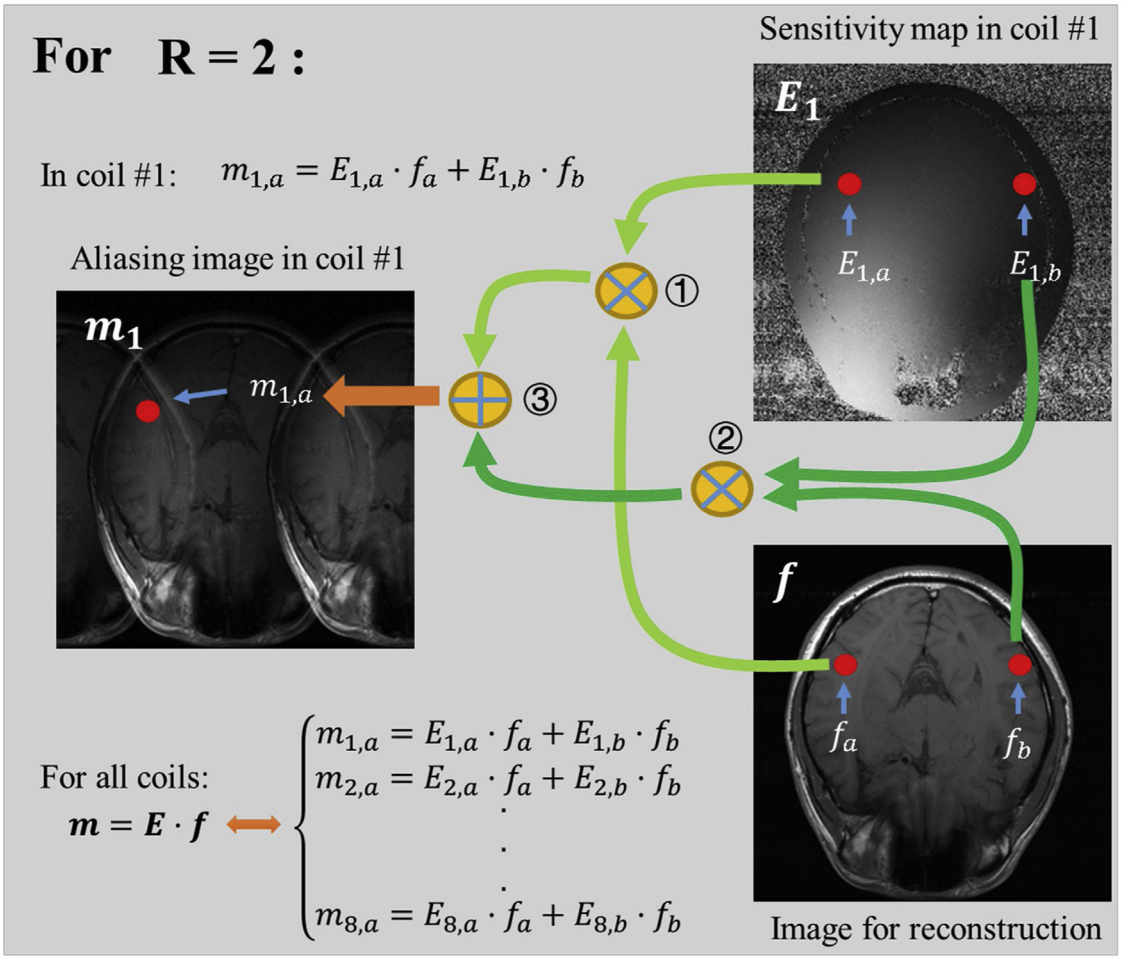

Fig. 3. Illustration for the simplest case in which reduction factor R = 2.

In Eq.4, matrix multiplication on the left side is equivalent to the linear equations on the right side. It can be generalized to all positions, which is Eq. (5).

$$\boldsymbol{m} = \boldsymbol{E}\boldsymbol{f} \tag{5}$$

Sensitivity maps (**E**) can be estimated and aliasing images (**m**) are received by surface coils. F_a and F_b are the unknown variables in Eq. (4). This is a common problem for solving overdetermined system in which the number of equations is greater than that of unknowns. A variety of optimization algorithms are mentioned in references [18,19] for solving the overdetermined system, and regularization is a way to correct the possible ill-posed problem. The method of least squares (given by Eq. (6)) can be used to find an approximate solution for Eq. (5). Moore–Penrose inverse matrix is used to calculate the unfolding matrix **U** [2] in Eq. (7).

$$\boldsymbol{f} = \arg\min_{f} \left\| \boldsymbol{m} - \boldsymbol{E}\boldsymbol{f} \right\|^2 \tag{6}$$

$$\boldsymbol{U} = \left(\boldsymbol{E}^{\boldsymbol{H}}\boldsymbol{\varphi}^{-1}\boldsymbol{E}\right)^{-1}\boldsymbol{E}^{\boldsymbol{H}}\boldsymbol{\varphi}^{-1} \tag{7}$$

Where superscript $\boldsymbol{H}$ indicates a matrix transpose, -1 means inverse. Matrix $\boldsymbol{\varphi}$ has one row and one column for each hybrid encoding carried out. Each diagonal entry represents the variance of noise in the corresponding sample value, while the off-diagonal elements reflect noise correlation between samples. In weak voxel conditions described in [2], $\boldsymbol{\varphi}$ can be omitted to simplify Eq. (7). It is practical when sampling k-space with regular Cartesian trajectories though it is time-consuming. The situation turns to be more complicated with other k-space trajectories, such as spirals or radial schemes. Solving Eq. (7) in a straightforward matrix inverse calculation requires numerical cost. The possible existence of ill condition in Eq. (7) may also lead to unsatisfactory reconstruction.

Iterative solving method using conjugate gradient (CG) algorithm is proposed to approximate the image optimally [20]. To satisfy the safely positive-definite requirement of CG and improve the speed of convergence in iterations, density and intensity correction are introduced to Eq. (8), and the problem of solving Eq. (6) can be approximately taken place by Eq. (9):

$$\tilde{\boldsymbol{U}} = \left(\boldsymbol{I}\boldsymbol{E}^{\boldsymbol{H}}\boldsymbol{D}\boldsymbol{E}\boldsymbol{I}\right)^{-1}\boldsymbol{I}\boldsymbol{E}^{\boldsymbol{H}}\boldsymbol{D} \tag{8}$$

$$\boldsymbol{f} = \tilde{\boldsymbol{U}} \cdot \boldsymbol{m} = \left(\boldsymbol{I}\boldsymbol{E}^{\boldsymbol{H}}\boldsymbol{D}\boldsymbol{E}\boldsymbol{I}\right)^{-1}\boldsymbol{I}\boldsymbol{E}^{\boldsymbol{H}}\boldsymbol{D}\boldsymbol{m} \tag{9}$$

In which **I** denotes the intensity matrix and **D** is for density correction. Thus, to solve the optimal solution Eq. (9), the first order derivative of $\boldsymbol{f}$ should be 0, given by Eq. (10):

$$\boldsymbol{I}\boldsymbol{E}^{\boldsymbol{H}}\boldsymbol{D}\boldsymbol{m} - \left(\boldsymbol{I}\boldsymbol{E}^{\boldsymbol{H}}\boldsymbol{D}\boldsymbol{E}\boldsymbol{I}\right)\left(\boldsymbol{I}^{-1}\boldsymbol{f}\right) = 0 \tag{10}$$

Density correction is determined by k-space sampling pattern and intensity correction is performed by the inverse sum of squares of sensitivity in each coil, which is associated with the encoding matrix **E**. The accurate estimation of coil sensitivity plays a key role in solving Eq. (10).

In methods of SENSE-like, the reconstruction is based on image domain. The sensitivity is derived in a way of dividing each coil aliasing image by their sum of squares combination. Error without removal in estimation of sensitivity will propagate to imaging.

Table 1
Formulae discussed in this work.

Step	formula	environment
To calculate the actual sampled lines in K-space	$\mathrm{SUM} = N^{ACSL} + \frac{N^{fully\ sampled} - N^{ACSL}}{R_{nom}}$	Developed in Matlab
To calculate the actual accelerating speed	$R_{net} = \frac{N^{fully\ sampled}}{SUM}$	Developed in Matlab
To calculate the normalized mean squared error NMSE	$\mathrm{NMSE} = \sum_{i}^{\mathrm{CoilN}} \frac{\lvert I_{recon}(i) - I_{sos}\rvert}{\lvert I_{sos}\rvert}$	Developed in Matlab
Each aliasing pixel in $\boldsymbol{m}_1$ is a superposition resulting from two pixels in $\boldsymbol{f}$	$m_{1,a} = E_{1,a} \cdot f_a + E_{1,b} \cdot f_b$	Theory Example
For all the eight coils, $m_{i,a}$ is the combination of $E_{i,a} \cdot f_a$ and $E_{i,b} \cdot f_b$, $i = 1, 2, \ldots 8$	$\boldsymbol{m_a} = \boldsymbol{E_a} \cdot \boldsymbol{f_a} \longleftarrow \begin{cases} m_{1,a} = E_{1,a} \cdot f_a + E_{1,b} \cdot f_b \\ m_{2,a} = E_{2,a} \cdot f_a + E_{2,b} \cdot f_b \\ \cdot \\ \cdot \\ \cdot \\ m_{8,a} = E_{8,a} \cdot f_a + E_{8,b} \cdot f_b \end{cases} \boldsymbol{m} = \boldsymbol{Ef}$	Developed in Matlab
Least square optimization. To reconstruct the low resolution image with ACS lines.	$\boldsymbol{f} = \arg\min_{f} \left\lvert \boldsymbol{m} - \boldsymbol{Ef} \right\rvert^2$	Developed in Matlab
Moore–Penrose inverse matrix which was used to calculate the unfolding matrix U	$\boldsymbol{U} = (\boldsymbol{E}^{\boldsymbol{H}} \boldsymbol{\varphi}^{-1} \boldsymbol{E})^{-1} \boldsymbol{E}^{\boldsymbol{H}} \boldsymbol{\varphi}^{-1}$	Developed in Matlab
Density and intensity correction	$\tilde{\boldsymbol{U}} = (\boldsymbol{IE}^{\boldsymbol{H}} \boldsymbol{DEI})^{-1} \boldsymbol{IE}^{\boldsymbol{H}} \boldsymbol{D}$	Developed in Matlab
Substitute $\boldsymbol{U}$ with $\tilde{\boldsymbol{U}}$	$\boldsymbol{f} = \tilde{\boldsymbol{U}} \cdot \boldsymbol{m} = (\boldsymbol{IE}^{\boldsymbol{H}} \boldsymbol{DEI})^{-1} \boldsymbol{IE}^{\boldsymbol{H}} \boldsymbol{Dm}$	Developed in Matlab
To solve $\boldsymbol{f}$, its first order derivative should be 0.	$\boldsymbol{IE}^{\boldsymbol{H}} \boldsymbol{Dm} - \left(\boldsymbol{IE}^{\boldsymbol{H}} \boldsymbol{DEI}\right) \left(\boldsymbol{I}^{-1} \boldsymbol{f}\right) = 0$	Developed in Matlab
Least square optimization. To estimate accurate coil sensitivity with the low resolution image $\boldsymbol{f}$.	$\boldsymbol{E} = \arg\min_{E} \boldsymbol{m} - \boldsymbol{Ef}^2$	Developed in Matlab
To solve $\boldsymbol{E}$, its first order derivative should be 0.	$\boldsymbol{f}^{\boldsymbol{H}} \boldsymbol{m} - \left(\boldsymbol{f}^{\boldsymbol{H}} \boldsymbol{f}\right) \boldsymbol{E} = 0$	Developed in Matlab
Least square optimization. Penalty objective function was built to utilize the prior information outside ROI.	$\{\boldsymbol{E}, \sigma\} = \arg\min_{\{\boldsymbol{E},\sigma\}} \left\{ \left\lvert \boldsymbol{m} - \boldsymbol{Ef} \right\rvert^2 + \sigma \lvert \boldsymbol{ME} \rvert^2 \right\}$	Developed in Matlab
To solve the penalty function above, its first order derivative should be 0.	$\boldsymbol{f}^{\boldsymbol{H}} \boldsymbol{m} - \left(\boldsymbol{f}^{\boldsymbol{H}} \boldsymbol{f} + \sigma \boldsymbol{M}\right) \boldsymbol{E} = 0$	Developed in Matlab

It is not enough to improve SNR and quality of image only by the processes of smoothing, low pass filtering or polynomial fitting. A separate calibration scan with full sampling k-space in SENSE prolongs time of imaging, although it maintains details of sensitivity and guarantees the quality of pMRI. To avoid this shortage, SC SENSE takes advantage of the characteristics that sensitivity changes slowly which is uniformly spatial distributed, and fully samples the phase encoding center lines in k-space to reconstruct low resolution reference images to accomplish estimation instead of an extra calibration scan. This method effectively saves scanning time while error is also enhanced with the loss of high frequency components in k-space.

To further improve the accuracy of sensitivity in each surface coil, sensitivity can be considered as an unknown with parameters to be solved. Low resolution images are used to combine an intermediate reference image using sum of squares. It is treated as an approximate reconstruction $\boldsymbol{f}$ using to estimate sensitivity $\mathbf{E}$ in the following objective function:

$$\boldsymbol{E} = \arg\min_{E} \left\| \boldsymbol{m} - \boldsymbol{Ef} \right\|^2 \tag{11}$$

$$\boldsymbol{f}^{\boldsymbol{H}} \boldsymbol{m} - \left(\boldsymbol{f}^{\boldsymbol{H}} \boldsymbol{f}\right) \boldsymbol{E} = 0 \tag{12}$$

Sensitivity estimation in regions outside the area of interest usually makes no sense for reconstruction. Theoretically the value should be zero. However, due to the presence of noise in space and surface coil in reality, it tends to be relatively small rather than zero. Zero-filling also makes sensitivity maps which are estimated from little lines in k-space to lose more information. On the basis of the above, penalty term instead of assignment can be added during optimal solving to suppress noise external to the region of interest. Sensitivity are multiplied by the mask matrix $\mathbf{M}$ which indicates the boundary of body and shares the same dimension with $\mathbf{m}$. The values in $\mathbf{M}$ in region of interest are assigned to 0, and others are set to 1. Therefore, during the process of iteration, signals coming from outside body region will be suppressed gradually.

$$\{\boldsymbol{E}, \sigma\} = \arg\min_{\{\boldsymbol{E},\sigma\}} \left\{ \left\| \boldsymbol{m} - \boldsymbol{Ef} \right\|^2 + \sigma \left\| \boldsymbol{ME} \right\|^2 \right\} \tag{13}$$

$$\boldsymbol{f}^{\boldsymbol{H}} \boldsymbol{m} - \left(\boldsymbol{f}^{\boldsymbol{H}} \boldsymbol{f} + \sigma \boldsymbol{M}\right) \boldsymbol{E} = 0 \tag{14}$$

M $\boldsymbol{M}$ can be obtained by edge detection of the intermediate low resolution image $\boldsymbol{f}$. Factor σ σ is positive which controls the degree

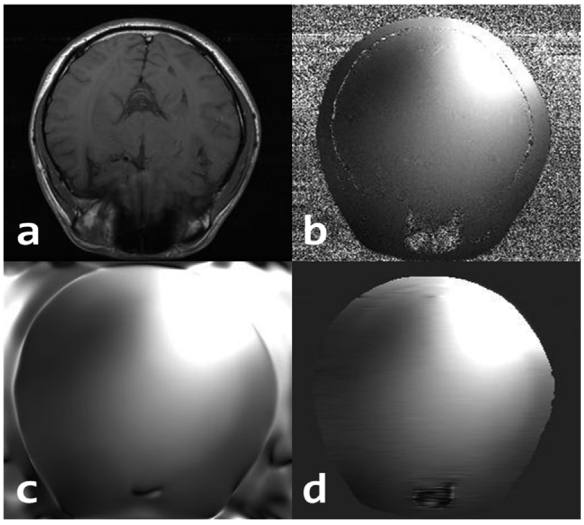

Fig. 4. Sensitivity maps of the fifth channel estimated to reconstruct image used by different methods. (a) the reference SoS brain image, (b) sensitivity maps based on full-scan data, (c) sensitivity maps estimated from the 32 ACS lines in k-space data, which are used in SC SENSE, and (d) sensitivity maps estimated by iterative solution with penalty term proposed in this paper. The penalty factor is set to 1 and the threshold is 0.1.

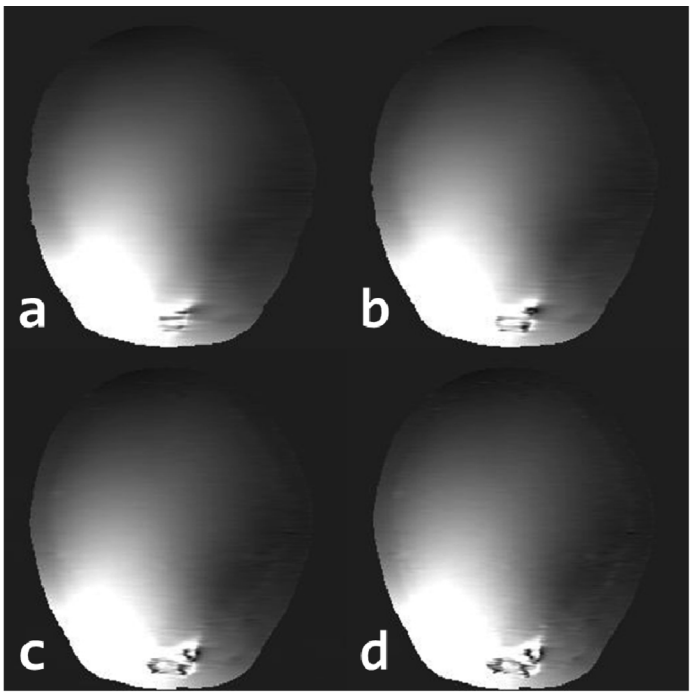

Fig. 5. Sensitivity maps of the first channel iterative solved by (a) ACS line = 24, (b) ACS line = 32, (c) ACS line = 48, and (d) ACS line = 64.

Fig. 5. Sensitivity maps of the first channel iterative solved by (a) ACS line = 24, (b) ACS line = 32, (c) ACS line = 48, and (d) ACS line = 64.

of penalty, and the appropriate one will be determined by solving the external penalty function [21].

All the formulae discussed in this work are summarized in following table (Table 1).

3. Results

The reconstructed brain image using SoS method is shown in Fig. 4a. As a standard reference, the corresponding sensitivity maps of the fifth channel based on the full scan data are shown in Fig. 4b. It can be observed that noise in the background emerge as a part of sensitivity. Fig. 4c-d show the estimated sensitivity maps by using SC SENSE and the proposed method in this paper. In the SC method, low resolution images produced by 2D-iFFT from 32 ACS lines in k-space of each channel are divided by the SoS combination to derive the sensitivity maps, noises outside the body take part in reconstructing the pMRI, as low frequency signals. It is propagated to result in various errors in the final image. Fig. 4d shows the result of iterative solution with a penalty term to restrain errors outside body rather than multiplying mask with the image.

Fig. 5a–d show the sensitivity maps of the first channel estimated by iterative solution. Center lines of phase encoding direction in k-space are sampled, and others are set to be zero. The more ACS lines used, the higher accuracy can be achieved, which results in better SNR in pMRI. However, sampling more ACS lines means requirement of more scanning time, so there is a tradeoff between imaging speed and quality. In iteration, penalty factor and threshold also impact the convergence speed. Fig. 6 illustrates the iteration times with various levels of penalty factor. Penalty factor is multiplied by penalty term in the objective function, so a larger value represents a more severe punishment outside the body by giving the prior knowledge about the region of interest (ROI).

Fig. 7a-f show comparisons between the SC SENSE and the method proposed in this paper with reduction factor = 3 and ACS lines = 32. Visually both them produce reconstruction without obvious artifacts, while in SC SENSE, noises can be seen clearly somewhere. The regional enlarged views with magnified image are shown in Fig. 7b and e, corresponding to the dotted region marked in Fig.7a and d. Fig.7c and f show the difference maps of the two methods respectively with the SoS reconstruction as a reference. Reconstruction errors are plotted in white. Sensitivity maps under iterative solution proposed in this paper depress the propagation of error and finally improve the quality of reconstruction.

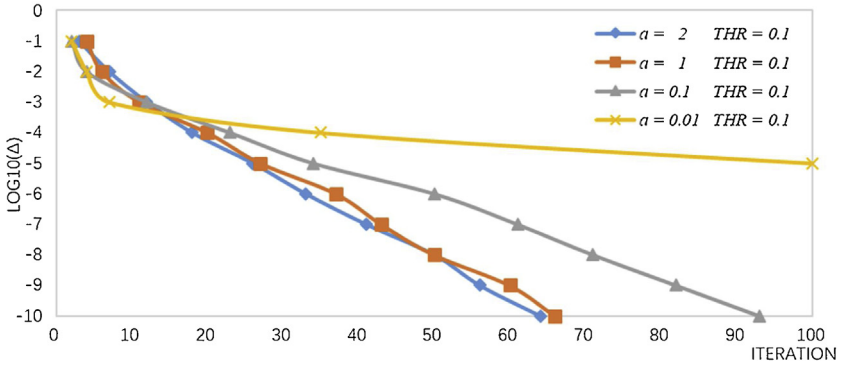

Fig. 6. Convergence speed vs. penalty factor. Axis X represents the logarithmic plots of the true image error (Δ) as functions of the iteration numbers (axis Y) in the iterative sensitivity maps estimation.

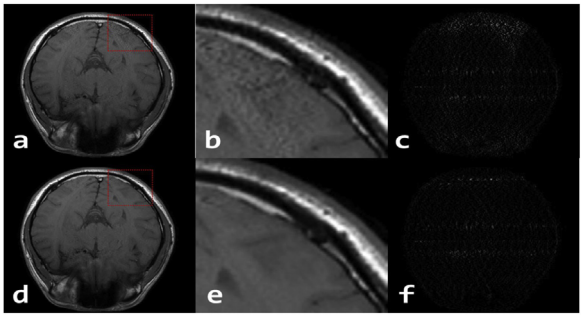

Fig. 7. Comparison of the reconstruction results from a set of 8 channels with reduction factor = 3 and ACS lines = 32. The first row shows the results using SC SENSE. (a) the reconstructed brain image, (b) regional enlarged view of (a) marked in dotted line, and (c) the difference map between SC SENSE and SoS reconstruction. The second row shows the results using the method proposed in this paper. (d) the reconstructed brain image, (e) regional enlarged view of (d) marked in dotted line, and (f) the difference map between the method proposed and SoS reconstruction.

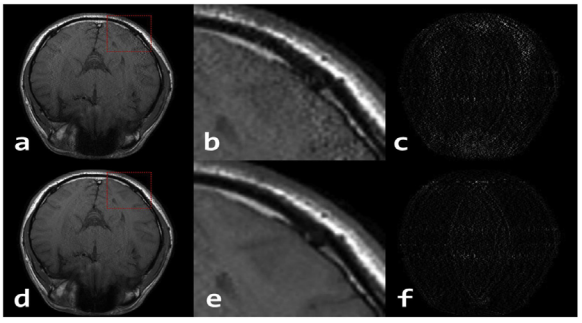

Fig. 8. Comparison of the reconstruction results from a set of 8 channels with reduction factor = 4 and ACS lines = 32. The other parameters are set to be the same with Fig. 7.

The same set of comparison for reduction factor = 4 and ACS lines = 32 are given in Fig. 8. The results also agree to the fact that the method proposed achieves better parallel MR imaging than SC SENSE.

4. Discussion

The method proposed takes advantages of SC SENSE and JSENSE, and fully makes the best of prior knowledge that sensitivity maps outside take little effect on the reconstruction. Two aspects of improvement are addressed. First, joint sensitivity estimation and image reconstruction is achieved by using the intermediate images in each coil, which avoids repeating the whole process of refining sensitivity maps. Second, penalty term is added to the optimal solving to make sensitivity estimation closer to reality instead of zero-filling in the region outside the object. The mask matrix **M** can be obtained by numerous methods based on the edge extraction of the region of interest. In this paper, it is simply completed by gradient calculating to detect where the boundary locates in the low resolution image reconstructed by SoS. For complicated situations, advanced techniques should be introduced to mark the region properly.

Table 2 and Fig. 9 illustrate the comparison of NMSEs between the proposed method and SC SENSE reconstruction. Different situations are taken into account with varied reduction factor and number of ACS lines. The penalty factor (σ) here is set to be 1 and threshold (T) is 0.1. From the curves plotted, they demonstrate the superior image quality of iterative solution with prior knowledge in sensitivity estimation, while error and noise are suppressed in iterations. For small reduction factors, such as 2 or 3, the quality of reconstructed image is almost as well as the SoS reconstruction. While, as it raises to 4 or 5, or even higher, the differences are distinguished. The dotted region marked in Fig. 9 is magnified in Fig. 10 to clearly observe NMSEs. For the reduction factor of 4 alone, axis X is changed to ACS lines. The results coincide with common sense that more ACS lines sampled in k-space enhance the details of sensitivity maps and improve the quality of reconstruction no matter what method is adopted. Because of the errors in sensitivity maps of the

Table 2
$NMSE_S$ of reconstructions from brain data.

$\sigma = 1$, T = 0.1															
ACS	$R_{nom} = 2$			$R_{nom} = 3$			$R_{nom} = 4$			$R_{nom} = 5$			$R_{nom} = 6$		
	R_{net}	N (%)	S (%)	R_{net}	N (%)	S (%)	R_{net}	N (%)	S (%)	R_{net}	N (%)	S (%)	R_{net}	N (%)	S (%)
24	1.83	0.05	0.07	2.53	0.10	0.22	3.12	0.27	0.66	3.64	1.00	3.90	4.09	7.91	15.15
32	1.78	0.04	0.06	2.40	0.09	0.20	2.91	0.22	0.61	3.33	0.77	3.56	3.69	6.33	14.48
48	1.68	0.04	0.05	2.18	0.08	0.17	2.56	0.18	0.51	2.86	0.58	3.13	3.10	4.62	13.25
64	1.60	0.03	0.04	2.00	0.07	0.15	2.29	0.16	0.44	2.50	0.48	2.78	2.67	3.77	12.22

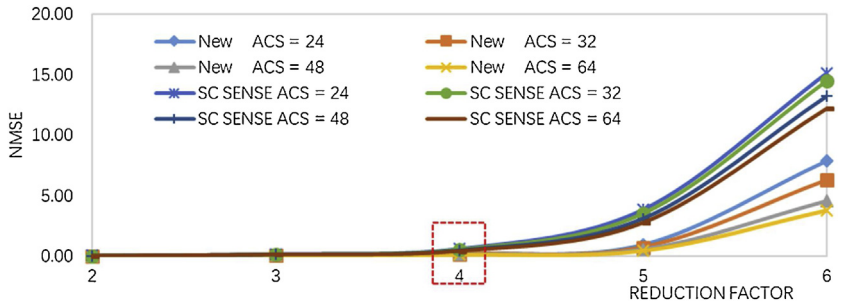

Fig. 9. NMSEs comparison between SC SENSE and the method we propose. Axis X represents the reduction factor ranging from 2 to 6, and the axis Y is the NMSE values. Different ACS lines (24\32\48\64) are sampled in experiments to compare the results of reconstruction. The curves illustrate the trend that NMSE values of the method proposed are less than SC SENSE, and demonstrate its superiority over SC SENSE.

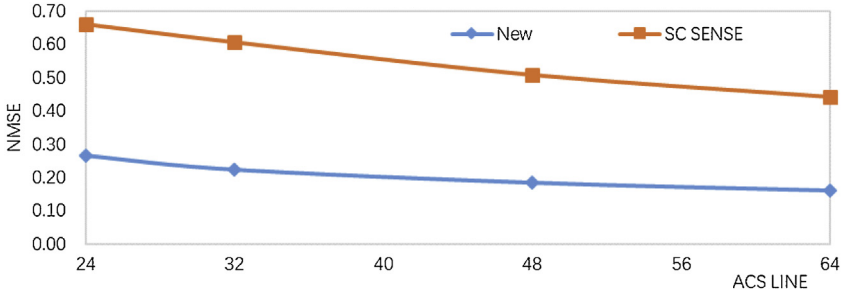

Fig. 10. NMSEs comparison between SC SENSE and the method proposed with reduction factor = 4. It is a magnification of the dotted region in Fig. 9.

independent estimation using SC SENSE, too much missing lines in k-space degrade the SNR and make it difficult to reconstruct the image. It means that when a rather large reduction factor is desired, the proposed method is more appropriate to achieve better results than SC SENSE.

Exterior penalty method is used to search the optimal solution from the unfeasible domain to the feasible. That means sensitivity estimation is approximated from the background to the object region by iterations. A proper initial penalty factor σ should be carefully chosen because the smaller leads to unsatisfactory estimation with slow convergence speed while the larger one increases computational complexity. Other alternate penalty methods can be considered such as barrier method (also known as interior penalty) or augmented Lagrangian method. A penalty term for non-smoothness may further be applied to refine sensitivity maps as a solution for the difficulty in determination of the polynomial fitting order.

5. Conclusions

We proposed a new method by adding the penalty term to the sensitivity estimation to improve reconstruction quality in pMRI. Prior knowledge about the information outside the region of interest makes it possible to refine sensitivity in iterations. The reconstruction effectively eliminates noise and artifacts especially under a large reduction factor condition, and the compared results exhibit the superiority of the method proposed compared to SC SENSE. The penalty function introduced here can be used in combination with most existing SC SENSE-like techniques, which implement self-calibration by extracting ACS lines.

Acknowledgments

This work is supported by the National Natural Science Foundation of China (Grant No. 61871168) and the Fundamental Research Funds of Hangzhou Dianzi University (KYS055618118).

References

[1] D.K. Sodickson, W.J. Manning, Simultaneous acquisition of spatial harmonics (SMASH): fast imaging with radiofrequency coil arrays, Magn. Reson. Med. 38 (1997) 591–603.
[2] K.P. Pruessmann, M. Weiger, M.B. Scheidegger, P. Boesiger, SENSE: sensitivity encoding for fast MRI, Magn. Reson. Med. 42 (1999) 952–962.
[3] W.E. Kyriakos, L.P. Panych, D.F. Kacher, C.-F. Westin, S.M. Bao, R.V. Mulkern, F.A. Jolesz, Sensitivity profiles from an array of coils for encoding and reconstruction in parallel (SPACE RIP), Magn. Reson. Med. 44 (2000) 301–308.
[4] M.A. Griswold, P.M. Jakob, M. Nittka, J.W. Goldfarb, A. Haase, Partially parallel imaging with localized sensitivities (PILS), Magn. Reson. Med. 44 (2000) 602–609.
[5] M.A. Griswold, P.M. Jakob, R.M. Heidemann, M. Nittka, V. Jellus, J. Wang, B. Kiefer, A. Haase, Generalized autocalibrating partially parallel acquisitions (GRAPPA), Magn. Reson. Med. 47 (2002) 1202–1210.
[6] P.M. Jakob, M.A. Grisowld, R.R. Edelman, D.K. Sodickson, AUTO-SMASH: a self-calibrating technique for SMASH imaging, magnetic resonance materials in physics, Biol. Med. 7 (1998) 42–54.
[7] R.M. Heidemann, M.A. Griswold, A. Haase, P.M. Jakob, VD-AUTO-SMASH imaging, Magnet. Reson. Med. 45 (2001) 1066–1074.
[8] C.A. McKenzie, E.N. Yeh, M.A. Ohliger, M.D. Price, D.K. Sodickson, Self-calibrating parallel imaging with automatic coil sensitivity extraction, Magn. Reson. Med. 47 (2002) 529–538.
[9] M. Uecker, P. Lai, M.J. Murphy, P. Virtue, M. Elad, J.M. Pauly, S.S. Vasanawala, M. Lustig, ESPIRiT—an eigenvalue approach to autocalibrating parallel MRI: where SENSE meets GRAPPA, Magn. Reson. Med. 71 (2014) 990–1001.
[10] L. Ying, J. Sheng, Joint image reconstruction and sensitivity estimation in SENSE (JSENSE), Magn. Reson. Med. 57 (2007) 1196–1202.
[11] J. Lyu, U. Nakarmi, D. Liang, J. Sheng, L. Ying, KerNL: kernel-based NonLinear approach to parallel MRI reconstruction, IEEE Trans. Med. Imaging (2018).
[12] G. Xie, Y. Song, C. Shi, X. Feng, H. Zheng, D. Weng, B. Qiu, X. Liu, Accelerated magnetic resonance imaging using the sparsity of multi-channel coil images, Magn. Reson. Imaging 32 (2014) 175–183.
[13] M. Uecker, T. Hohage, K.T. Block, J. Frahm, Image reconstruction by regularized nonlinear inversion—joint estimation of coil sensitivities and image content, Magn. Reson. Med. 60 (2008) 674–682.
[14] I.Y. Chun, B. Adcock, T.M. Talavage, Efficient compressed sensing SENSE pMRI reconstruction with joint sparsity promotion, IEEE Trans. Med. Imaging 35 (2016) 354–368.
[15] J. Sheng, E. Wiener, B. Liu, F. Boada, L. Ying, Improved self-calibrated spiral parallel imaging using JSENSE, Med. Eng. Phys. 31 (2009) 510–514.
[16] S.A. Qazi, S. Nasir, A. Saeed, H. Omer, Optimizing Image Reconstruction in SENSE Using GPU, Applied Magnetic Resonance. (n.d.) 1–14.
[17] R.M. Heidemann, M.A. Griswold, N. Seiberlich, M. Nittka, S.A. Kannengiesser, B. Kiefer, P.M. Jakob, Fast method for 1D non-cartesian parallel imaging using GRAPPA, Magn. Reson. Med. 57 (2007) 1037–1046.

[18] K.P. Pruessmann, M. Weiger, P. Börnert, P. Boesiger, Spiral SENSE: Sensitivity Encoding With Arbitrary k-space Trajectories, 1999, pp. 94.
[19] S. Fang, L. Li, W. Wu, J. Wei, B. Zhang, D.-H. Kim, C. Yuan, H. Guo, Multiscale coherence regularization reconstruction using a nonlocal operator for fast variable-density spiral imaging, Magn. Reson. Imaging 34 (2016) 964–973.
[20] K.P. Pruessmann, M. Weiger, P. Börnert, P. Boesiger, Advances in sensitivity encoding with arbitrary k-space trajectories, Magn. Reson. Med. 46 (2001) 638–651.
[21] J. Viswanathan, I.E. Grossmann, A combined penalty function and outer-approximation method for MINLP optimization, Comput. Chem. Eng. 14 (1990) 769–782.